**Showcasing research from Professor Kudo's laboratory, Department of Applied Chemistry, Tokyo University of Science, Tokyo, Japan.**

Highly crystalline $Na_{0.5}Bi_{0.5}TiO_3$ of a photocatalyst valence-band-controlled with Bi(III) for solar water splitting

A highly crystalline $Na_{0.5}Bi_{0.5}TiO_3$ powder with a perovskite structure was successfully synthesized using a NaCl-flux method. The powdered photocatalyst in which the valence band consisted of Bi(III) showed a 5.1% apparent quantum yield at 350 nm for water splitting.
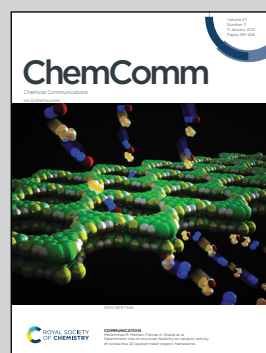
ROYAL SOCIETY OF CHEMISTRY

rsc.li/chemcomm

ChemComm

Check for updates

Highly crystalline $Na_{0.5}Bi_{0.5}TiO_3$ of a photocatalyst valence-band-controlled with Bi(III) for solar water splitting†

Kenta Watanabe, [a] Yoichi Iikubo,[a] Yuichi Yamaguchi[ab] and Akihiko Kudo ⭑[ab]

$Na_{0.5}Bi_{0.5}TiO_3$ (BG 3.1 eV) with a valence band formed by Bi(III) was found as a new photocatalyst for solar water splitting. The water splitting activity of highly crystalline $Na_{0.5}Bi_{0.5}TiO_3$ synthesized by a flux method was much higher than that of the samples synthesized by a solid-state reaction. The optimized $RhCr_2O_x$(0.1 mol%)/$Na_{0.5}Bi_{0.5}TiO_3$/CoOOH(0.02 mol%) gave a 5.1% apparent quantum yield at 350 nm and split water even under simulated sunlight irradiation with a 0.05% solar to hydrogen energy conversion efficiency. We have successfully achieved solar water splitting using a one-step photoexcitation type photocatalyst valence-band-controlled with Bi(III).

Hydrogen production by photocatalytic solar water splitting is attractive, and important science and technology from the viewpoint of resource, energy and environmental issues. Therefore, many researchers have developed various powder-based visible-light-driven photocatalysts working by a one-step photoexcitation and a Z-schematic two-step photoexcitation for water splitting.[1–6] The one-step photoexcitation type photocatalyst especially possesses an advantage in practical use from the viewpoint of its simplicity. Domen and co-workers have reported that GaN–ZnO,[7] $ZnGeN_2$–ZnO,[8] $LaMg_{1/3}Ta_{2/3}O_2N$,[9] TaON,[10] $CaTaO_2N$,[11] Ta_3N_5[12] and $Y_2Ti_2O_5S_2$[13] of (oxy)nitride and oxysulfide photocatalysts show activities for one-step photoexcitation type water splitting under visible light irradiation. It is also reported that g-C_3N_4 of an organic semiconductor photocatalyst can split water under visible light irradiation.[14] We have also reported that IrO_2-loaded $SrTiO_3$ co-doped with Rh and Sb of a metal oxide photocatalyst shows activity for water splitting under visible light irradiation.[15] Although some

of these visible-light-driven photocatalysts can split water under simulated sunlight irradiation, their solar to hydrogen energy conversion efficiencies (STH) are still low due to their low apparent quantum yields (AQYs). In recent years, Domen and co-workers have developed an Al-doped $SrTiO_3$ (band gap (BG) 3.2 eV) photocatalyst loading Rh/Cr_2O_3 and CoOOH cocatalysts with almost 100% AQY, which was prepared by a flux treatment.[16] Although the photocatalyst responds to only UV light, it shows the highest STH (0.65%) among one-step photoexcitation type photocatalysts.[16] We have also reported that $Rh_{0.5}Cr_{1.5}O_3$-loaded $AgTaO_3$ (BG 3.4 eV) shows high AQY (38% at 340 nm) and STH (0.13%) for water splitting.[17] The valence band maximum (VBM) of the Al-doped $SrTiO_3$ is formed by O2p orbitals, while that of $AgTaO_3$ is formed by Ag4d orbitals.[18] A photocatalyst whose valence band (VB) is formed by orbitals of elements except oxygen like $AgTaO_3$ is called a valence-band (VB)-controlled photocatalyst.[3,17,19] The VB-controlled photocatalyst is very important from the viewpoint of extension of responsive wavelength. Although the STH of the $Rh_{0.5}Cr_{1.5}O_3$-loaded $AgTaO_3$ is the highest among the VB-controlled photocatalysts, the BG of the $AgTaO_3$ is wider than that of the Al-doped $SrTiO_3$. Therefore, it is important to achieve solar water splitting with high STH using a VB-controlled photocatalyst with a narrower BG than the Al-doped $SrTiO_3$.

$Na_{0.5}Bi_{0.5}TiO_3$ (BG 3.1 eV) with a perovskite structure is one of the candidates satisfying the conditions mentioned above, because Bi(III) is a suitable cation for the VB-controlled photocatalyst, as seen in $BiVO_4$, $Na_{0.5}Bi_{0.5}WO_4$ and $Bi_4Ti_3O_{12}$.[20–22] The VB of $Na_{0.5}Bi_{0.5}TiO_3$ is formed by hybridized orbitals consisting of O2p and Bi6s, leading to the narrower BG than $SrTiO_3$.[23] $Na_{0.5}Bi_{0.5}TiO_3$ showed activities for photocatalytic H_2 and O_2 evolution from aqueous solutions containing sacrificial reagents under UV irradiation as half reactions of water splitting.[24,25] $Na_{0.5}Bi_{0.5}TiO_3$ photocatalysts have also been used for degradation of dyes.[26,27] However, water splitting into H_2 and O_2 at a stoichiometric ratio over the $Na_{0.5}Bi_{0.5}TiO_3$ has not been achieved yet. The distortion of the perovskite framework in the crystal structure of $Na_{0.5}Bi_{0.5}TiO_3$ is similar to that of

a Department of Applied Chemistry, Faculty of Science, Tokyo University of Science, 1-3 Kagurazaka, Shinjuku-ku, Tokyo 162-8601, Japan. E-mail: a-kudo@rs.tus.ac.jp

b Photocatalysis International Research Center, Research Institute for Science and Technology, Tokyo University of Science, 2641 Yamazaki Noda-Shi, Chiba-ken 278-8510, Japan

† Electronic supplementary information (ESI) available: Experimental detail, crystal structure, XRD, XRF, XPS, DRS and a time course of an activity. See DOI: 10.1039/d0cc07371g

Communication

View Article Online

ChemComm

AgTaO$_3$ (Fig. S1 and Table S1, ESI†). Therefore, Na$_{0.5}$Bi$_{0.5}$TiO$_3$ is expected to possess potential for photocatalytic water splitting. Moreover, the activity of Na$_{0.5}$Bi$_{0.5}$TiO$_3$ will be improved by changing the synthesis method from a conventional solid state reaction to a flux method as well as that of SrTiO$_3$[28] because Na$_{0.5}$Bi$_{0.5}$TiO$_3$ is similar to SrTiO$_3$ from the viewpoints of a perovskite structure consisting of TiO$_6$ octahedra. A flux method is useful to control bulk properties of a material such as morphology and crystallinity.[29–32] In the present study, we synthesized Na$_{0.5}$Bi$_{0.5}$TiO$_3$ of a photocatalyst VB-controlled with Bi6s orbitals by a solid state reaction and a flux method, and investigated their photocatalytic water splitting with loading suitable cocatalysts.

Na$_{0.5}$Bi$_{0.5}$TiO$_3$ was synthesized by a solid state reaction (SSR) and a flux method (FM) using Na$_2$CO$_3$ (Kanto Chemical; 99.8%), Bi$_2$O$_3$ (Kanto Chemical; 99.9%) and TiO$_2$ (Kojundo; 99.99%) as starting materials. After the starting materials were mixed in an alumina mortar in a ratio of Na$_2$CO$_3$: Bi$_2$O$_3$: TiO$_2$ = 0.25 : 0.25 : 1, the mixture was calcined at 1173–1373 K for 5 h in air for the SSR. The obtained material was washed with distilled water. For the FM, 10 molar equivalence of NaCl (Kanto Chemical; 99.5%) to the objective was used as a flux reagent. The mixture of the starting materials and the NaCl-flux was heated at 1173–1473 K for 5 h in air. The obtained material was washed with distilled water to remove the NaCl-flux. Na$_{0.5}$La$_{0.5}$TiO$_3$ and Na$_{0.5}$La$_{0.25}$Bi$_{0.25}$TiO$_3$ were also synthesized by FM at 1273 K for 5 h with the NaCl-flux in order to compare their band structures with Na$_{0.5}$Bi$_{0.5}$TiO$_3$. Details of the experiment are described in the footnotes of the Figures and Tables, and the ESI.†

X-ray diffraction (XRD) patterns revealed that Na$_{0.5}$Bi$_{0.5}$TiO$_3$ was successfully synthesized by SSR and FM (Fig. S2, ESI†). The FWHMs of the (012) peaks of the sample synthesized by FM at 1273–1473 K were similar to each other and smaller than those of the other samples. This result indicates that these samples synthesized by FM at 1273–1473 K possessed higher crystallinity than the other samples. The change in width of the peak split between (104) and (110) depending on the calcination temperature suggests that distortion of the perovskite framework slightly changed. The effect of synthesis method on the morphology of Na$_{0.5}$Bi$_{0.5}$TiO$_3$ particles was investigated by scanning electron microscopy (SEM) measurements, as shown in Fig. 1. The particle surfaces of the samples synthesized by FM were more faceted than those of the samples synthesized by SSR. Particles prepared by FM were small comparing with SSR at the same calcination temperature. The surface area (S.A.) of the samples synthesized by FM was larger than those of the samples synthesized by SSR. All absorption edges of diffuse reflectance spectra (DRS) of the Na$_{0.5}$Bi$_{0.5}$TiO$_3$ were located at around 400–420 nm, as shown in Fig. 2, indicating that the BG of Na$_{0.5}$Bi$_{0.5}$TiO$_3$ was 3.0–3.1 eV. The BG of Na$_{0.5}$La$_{0.5}$TiO$_3$ in which the VB is formed by O2p orbitals was estimated to be 3.4 eV from its DRS. Therefore, the BG of Na$_{0.5}$Bi$_{0.5}$TiO$_3$ was narrowed about 0.3 eV due to the contribution of Bi6s orbitals to its VB. The absorption edge of Na$_{0.5}$La$_{0.25}$Bi$_{0.25}$TiO$_3$ was located between those of the Na$_{0.5}$La$_{0.5}$TiO$_3$ and the Na$_{0.5}$Bi$_{0.5}$TiO$_3$ (Fig. S3, ESI†). XPS spectra at the VB regions of
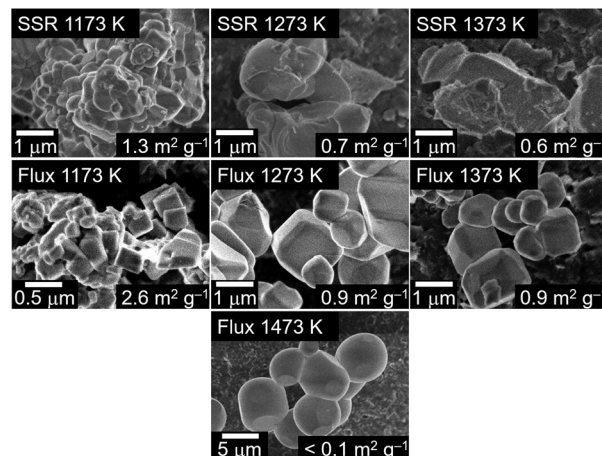

Fig. 1 SEM images and surface areas of Na$_{0.5}$Bi$_{0.5}$TiO$_3$ synthesized by SSR and FM at various temperatures.

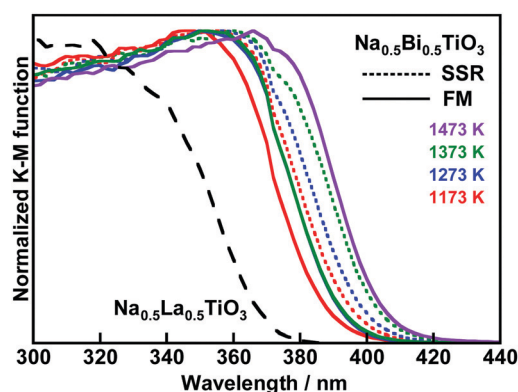**Fig. 2** Diffuse reflectance spectra of Na$_{0.5}$Bi$_{0.5}$TiO$_3$ synthesized by SSR and FM at various temperatures and Na$_{0.5}$La$_{0.5}$TiO$_3$ synthesized by FM at 1273 K.

Na$_{0.5}$Bi$_{0.5}$TiO$_3$ and Na$_{0.5}$La$_{0.5}$TiO$_3$ synthesized by FM at 1273 K were measured (Fig. S4, ESI†). The peak of the Na$_{0.5}$Bi$_{0.5}$TiO$_3$ was wider than that of the Na$_{0.5}$La$_{0.5}$TiO$_3$. The onset binding energy of the peak of the Na$_{0.5}$Bi$_{0.5}$TiO$_3$ shifted to a lower energy of about 0.3 eV than that of the Na$_{0.5}$La$_{0.5}$TiO$_3$. These results also suggest that Bi6s orbitals contributed to the valence band maximum (VBM) of the Na$_{0.5}$Bi$_{0.5}$TiO$_3$. DFT calculations also revealed that Bi(III) contributed to the VB of the Na$_{0.5}$Bi$_{0.5}$TiO$_3$.[23] The VBM formed by O2p orbitals of materials consisting of MO$_6$ (M = metal cation) such as Na$_{0.5}$La$_{0.5}$TiO$_3$ are located around +3.0 eV *vs.* RHE.[33] Thus, the conduction band minimum (CBM) of Na$_{0.5}$La$_{0.5}$TiO$_3$ was calculated to be −0.4 eV *vs.* RHE from its BG. CBM depends on the distortion of M–O–M bond angles.[34] Therefore, the CBM of Na$_{0.5}$Bi$_{0.5}$TiO$_3$ was also −0.4 eV *vs.* RHE because the Ti–O–Ti bond angle of the Na$_{0.5}$Bi$_{0.5}$TiO$_3$ was similar to that of the Na$_{0.5}$La$_{0.5}$TiO$_3$ (Table S1, ESI†). The CBM of Na$_{0.5}$Bi$_{0.5}$TiO$_3$ has an advantage in a driving force for reduction of water to hydrogen compared with that of SrTiO$_3$ (−0.2 V *vs.* RHE). The BG of the Na$_{0.5}$Bi$_{0.5}$TiO$_3$ was narrowed 0.3 eV by the contribution of Bi6s to its VBM compared with

$Na_{0.5}La_{0.5}TiO_3$, as mentioned above. The VBM of the $Na_{0.5}Bi_{0.5}TiO_3$ was calculated to be +2.7 eV from its BG and CBM. The small shift in the absorption edges seemed to be due to the difference in the distortion of the crystal structure and the particle size depending on the synthesis conditions. Additionally, the molar ratios of Bi/Ti for the samples synthesized by FM at 1173–1373 K were slightly smaller than those for the other samples (Table S2, ESI†). The smaller molar ratios of Bi/Ti for the samples synthesized by FM at 1173–1373 K also seemed to affect the difference in the absorption edges because Bi6s orbitals contributed to the VBM of $Na_{0.5}Bi_{0.5}TiO_3$.

Photocatalytic water splitting over $Na_{0.5}Bi_{0.5}TiO_3$ under UV irradiation ($\lambda > 300$ nm) was examined, as shown in Table 1. $RhCr_2O_x$ is an excellent cocatalyst for water splitting.[35,36] We applied the cocatalyst to the present $Na_{0.5}Bi_{0.5}TiO_3$. All samples produced H_2 and O_2 in a stoichiometric ratio. The samples synthesized by FM at 1273 and 1373 K especially showed high photocatalytic activities, because these samples possessed good crystallinity as seen in XRD (Fig. S2, ESI†). Photogenerated carriers easily migrated to the surface of such well-crystallized particles, resulting in high activities. Although the sample synthesized by FM at 1473 K possessed similar crystallinity to the samples synthesized by FM at 1273 and 1373 K, it showed a quite low activity because of its very small S.A. (<0.1 m^2 g^{-1}). Non-loaded $Na_{0.5}Bi_{0.5}TiO_3$ synthesized by FM at 1273 K hardly showed photocatalytic activity for water splitting under UV irradiation (Table S3, ESI†). 0.1 mol% was the optimum loading amount of the $RhCr_2O_x$ cocatalyst. Coloading of the $RhCr_2O_x$ cocatalyst with a CoOOH of an O_2-evolving cocatalyst is effective for water splitting over the Al-doped $SrTiO_3$ photocatalyst.[16,37] The water splitting activity of the $RhCr_2O_x$(0.1 mol%)-loaded $Na_{0.5}Bi_{0.5}TiO_3$ was further improved by loading of the CoOOH cocatalyst. $RhCr_2O_x$(0.1 mol%) and CoOOH(0.02 mol%)-coloaded $Na_{0.5}Bi_{0.5}TiO_3$ showed the highest activity for photocatalytic water splitting (Table S3 and Fig. S5, ESI†). The binding energy of the $Rh3d_{5/2}$ peak in the XPS spectrum of the $RhCr_2O_x$(0.1 mol%)/$Na_{0.5}Bi_{0.5}TiO_3$/CoOOH(0.02 mol%) (308.9 eV) was similar to not that of Rh_2O_3 (308.3 eV) but those of $Rh_{0.5}Cr_{1.5}O_3$(0.2 mol%)/$Na_{0.5}Bi_{0.5}TiO_3$ (308.9 eV) loaded by an impregnation method and previously reported $Rh_{2-x}Cr_yO_3$/
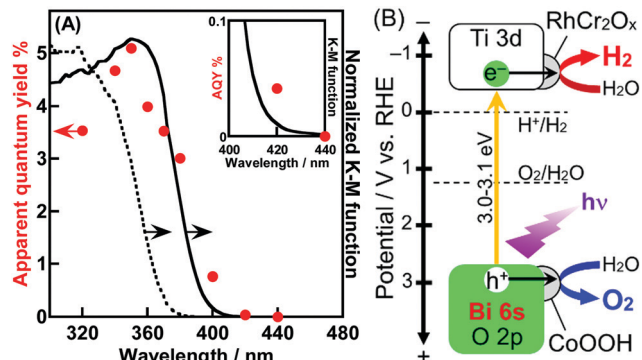

Fig. 3 (A) Action spectrum of photocatalytic water splitting over $RhCr_2O_x$(0.1 mol%)/$Na_{0.5}Bi_{0.5}TiO_3$/CoOOH(0.02 mol%), and diffuse reflectance spectra of $Na_{0.5}La_{0.5}TiO_3$ (dashed line) and $Na_{0.5}Bi_{0.5}TiO_3$ (solid line) synthesized by FM at 1273 K. Photocatalyst: 0.3 g, cocatalyst: PD, reactant solution: distilled water (120 mL), cell: top-irradiation cell with a Pyrex window, light source: 300 W Xe-arc lamp with band-pass filters. (B) Reaction scheme of photocatalytic water splitting over $RhCr_2O_x$(0.1 mol%)/$Na_{0.5}Bi_{0.5}TiO_3$/CoOOH(0.02 mol%).

$(Ga_{1-x}Zn_x)(N_{1-x}O_x)$ (309.0 eV) loaded by a simultaneous PD method (Fig. S6, ESI†).[35,36] Therefore, the $RhCr_2O_x$ loaded on the $Na_{0.5}Bi_{0.5}TiO_3$ was suggested to be mainly a $Rh_{2-y}Cr_yO_3$ of a mixed-oxide. The optimum $Na_{0.5}Bi_{0.5}TiO_3$ also showed much higher photocatalytic activity for water splitting than $Na_{0.5}La_{0.5}TiO_3$ and $Na_{0.5}La_{0.25}Bi_{0.25}TiO_3$ (Table S3, ESI†). This might be because photogenerated holes in the $Na_{0.5}Bi_{0.5}TiO_3$ could easily migrate to the particle surfaces because of the contribution of Bi(III) to the VB.

Fig. 3(A) shows an action spectrum of photocatalytic water splitting over the $RhCr_2O_x$(0.1 mol%)/$Na_{0.5}Bi_{0.5}TiO_3$/CoOOH(0.02 mol%). The onset wavelength of the activity agreed with that of the absorption spectrum of $Na_{0.5}Bi_{0.5}TiO_3$. This agreement indicates that water splitting proceeded with photoexcitation from the VB formed by Bi6s orbitals to the CB formed by Ti3d, as shown in Fig. 3(B). The AQY was 5.1% at 350 nm. As far as we know, among metal oxide photocatalysts with VB formed by Bi6s orbitals, the AQY is the highest for one-step photoexcitation type water splitting. Additionally, the AQY was slightly higher than that of $RhCrO_x$-loaded GaN–ZnO which shows the highest AQY among a visible-light-driven photocatalyst for water splitting.[7] Moreover, $RhCr_2O_x$(0.1 mol%)/$Na_{0.5}Bi_{0.5}TiO_3$/CoOOH(0.02 mol%) responded to light up to 420 nm.

Water splitting proceeded over the $RhCr_2O_x$(0.1 mol%)/$Na_{0.5}Bi_{0.5}TiO_3$/CoOOH(0.02 mol%) even under simulated sunlight irradiation, as shown in Fig. 4. H_2 and O_2 steadily evolved for a long time at the rates of 203 mL h^{-1} m^{-2} and 91 mL h^{-1} m^{-2}, respectively. The STH was estimated to be 0.05%. Thus, we successfully achieved one-step photoexcitation type solar water splitting using $RhCr_2O_x$(0.1 mol%)/$Na_{0.5}Bi_{0.5}TiO_3$/CoOOH(0.02 mol%) as a photocatalyst VB-controlled with Bi(III) possessing a narrower BG than $SrTiO_3$.

In conclusion, $Na_{0.5}Bi_{0.5}TiO_3$, which is a photocatalyst VB-controlled with Bi(III), synthesized by a flux method at 1273 K has arisen as a new photocatalyst for solar water splitting in a suspension system when $RhCr_2O_x$(0.1 mol%) and CoOOH(0.02 mol%) were coloaded. $Na_{0.5}Bi_{0.5}TiO_3$ synthesized

Table 1 Photocatalytic water splitting over $RhCr_2O_x$(0.2 mol%)-loaded $Na_{0.5}Bi_{0.5}TiO_3$ synthesized by SSR and FM under UV irradiation

Synthesis condition		FWHM of (012) peak/°	S. A./m^2 g^{-1}	Activity/μmol h^{-1}	
Method	Temp./K			H_2	O_2
SSR	1173	0.11	1.3	30	14
SSR	1273	0.10	0.7	33	16
SSR	1373	0.10	0.6	10	4.9
FM	1173	0.12	2.6	9	4
FM	1273	0.09	0.9	102	50
FM	1373	0.09	0.9	58	27
FM	1473	0.09	<0.1	1	0.4

Photocatalyst: 0.3 g, reactant solution: distilled water (120 mL), cell: top-irradiation cell with a Pyrex window, light source: 300 W Xe-arc lamp ($\lambda > 300$ nm). A $RhCr_2O_x$(0.2 mol%) cocatalyst was loaded *in situ* by a photodeposition (PD) method.

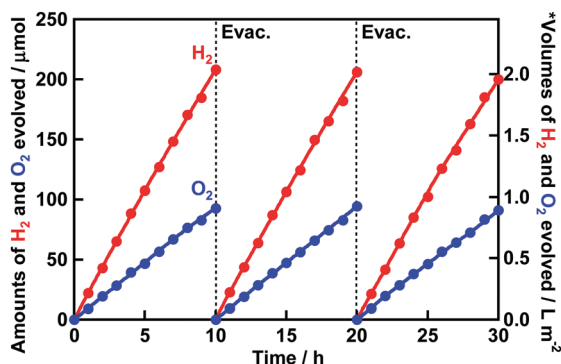**Fig. 4** Photocatalytic solar water splitting over $RhCr_2O_x$(0.1 mol%)/$Na_{0.5}Bi_{0.5}TiO_3$/CoOOH(0.02 mol%). $Na_{0.5}Bi_{0.5}TiO_3$ was synthesized by FM at 1273 K. Photocatalyst: 0.3 g, cocatalyst: PD, reactant solution: distilled water (120 mL), cell: top-irradiation cell with a Pyrex window, light source: solar simulator (AM-1.5 G, 100 mW cm^{-2}), irradiation area: 25 cm^2. *Volumes were calculated with the conditions of room temperature, supposing 1 atm and 1 m^2 of irradiated area.

by FM was more highly crystalized and faceted than the samples synthesized by SSR. XPS measurements revealed that the VBM of $Na_{0.5}Bi_{0.5}TiO_3$ was formed by Bi6s orbitals. The highly crystalline $Na_{0.5}Bi_{0.5}TiO_3$ with facets obtained by FM showed higher water splitting activity under UV irradiation than $Na_{0.5}Bi_{0.5}TiO_3$ obtained by SSR. This seemed to be because photogenerated carriers were able to easily migrate to the particle surfaces due to its high crystallinity. Optimized $RhCr_2O_x$(0.1 mol%)/$Na_{0.5}Bi_{0.5}TiO_3$/CoOOH(0.02 mol%) responded to light up to 420 nm. This photocatalyst gave 5.1% AQY at 350 nm and 0.05% STH. The AQY and STH were the highest among photocatalysts VB-controlled with Bi(III). Thus, we have demonstrated solar water splitting *via* one-step type photoexcitation using a VB-controlled photocatalyst consisting of Bi(III) with a narrower BG than $SrTiO_3$.

Conflicts of interest

There are no conflicts to declare.

References

1 F. E. Osterloh, *Chem. Mater.*, 2008, **20**, 35–54.
2 Y. Inoue, *Energy Environ. Sci.*, 2009, **2**, 364–386.
3 A. Kudo and Y. Miseki, *Chem. Soc. Rev.*, 2009, **38**, 253–278.
4 R. Abe, *J. Photochem. Photobiol., C*, 2010, **11**, 179–209.
5 T. Hisatomi, J. Kubota and K. Domen, *Chem. Soc. Rev.*, 2014, **43**, 7520–7535.
6 K. Maeda and K. Domen, *Bull. Chem. Soc. Jpn.*, 2016, **89**, 627–648.
7 K. Maeda, K. Teramura, D. Lu, T. Takata, N. Saito, Y. Inoue and K. Domen, *Nature*, 2006, **440**, 295.
8 Y. Lee, H. Terashima, Y. Shimodaira, K. Teramura, M. Hara, H. Kobayashi, K. Domen and M. Yashima, *J. Phys. Chem. C*, 2007, **111**, 1042–1048.
9 C. Pan, T. Takata, M. Nakabayashi, T. Matsumoto, N. Shibata, Y. Ikuhara and K. Domen, *Angew. Chem., Int. Ed.*, 2015, **54**, 2955–2959.
10 K. Maeda, D. Lu and K. Domen, *Chem. – Eur. J.*, 2013, **19**, 4986–4991.
11 J. Xu, C. Pan, T. Takata and K. Domen, *Chem. Commun.*, 2015, **51**, 7191–7194.
12 Z. Wang, Y. Inoue, T. Hisatomi, R. Ishikawa, Q. Wang, T. Takata, S. Chen, N. Shibata, Y. Ikuhara and K. Domen, *Nat. Catal.*, 2018, **1**, 756–763.
13 Q. Wang, M. Nakabayashi, T. Hisatomi, S. Sun, S. Akiyama, Z. Wang, Z. Pan, X. Xiao, T. Watanabe, T. Yamada, N. Shibata, T. Takata and K. Domen, *Nat. Mater.*, 2019, **18**, 827–832.
14 G. Zhang, Z.-A. Lan, L. Lin, S. Lin and X. Wang, *Chem. Sci.*, 2016, **7**, 3062–3066.
15 R. Asai, H. Nemoto, Q. Jia, K. Saito, A. Iwase and A. Kudo, *Chem. Commun.*, 2014, **50**, 2543–2546.
16 T. Takata, J. Jiang, Y. Sakata, M. Nakabayashi, N. Shibata, V. Nandal, K. Seki, T. Hisatomi and K. Domen, *Nature*, 2020, **581**, 411–414.
17 K. Watanabe, A. Iwase and A. Kudo, *Chem. Sci.*, 2020, **11**, 2330–2334.
18 H. Kato, H. Kobayashi and A. Kudo, *J. Phys. Chem. B*, 2002, **106**, 12441–12447.
19 A. Kudo, H. Kato and I. Tsuji, *Chem. Lett.*, 2004, **33**, 1534–1539.
20 A. Kudo, K. Omori and H. Kato, *J. Am. Chem. Soc.*, 1999, **121**, 11459–11467.
21 H. Kato, N. Matsudo and A. Kudo, *Chem. Lett.*, 2004, **33**, 1216–1217.
22 A. Kudo and S. Hijii, *Chem. Lett.*, 1999, 1103–1104.
23 M. Zeng, S. W. Or and H. L. W. Chan, *J. Appl. Phys.*, 2010, **107**, 043513.
24 Y. Iikubo, H. Kato and A. Kudo, *Abstract of 94th CATSJ Meeting, 2004, P038*; Y. Iikubo, MPhil thesis, Tokyo University of Science, 2005.
25 L. Wang and W. Wang, *Int. J. Hydrogen Energy*, 2012, **37**, 3041–3047.
26 Z. Ai, G. Lu and S. Lee, *J. Alloys Compd.*, 2014, **613**, 260–266.
27 R. Zhang, X. Wu, Y. Li, W. Shao, Y. Zhang, Z. Liu, J. Nie, J. Tan and W. Ye, *RSC Adv.*, 2020, **10**, 7443–7451.
28 Y. Ham, T. Hisatomi, Y. Goto, Y. Moriya, Y. Sakata, A. Yamakata, J. Kubota and K. Domen, *J. Mater. Chem. A*, 2016, **4**, 3027–3033.
29 X. Liu, N. Fechler and M. Antonietti, *Chem. Soc. Rev.*, 2013, **42**, 8237–8265.
30 Q. Wang, Q. Guo, L. Wang and B. Li, *Dalton Trans.*, 2016, **45**, 17748–17758.
31 Q. Wang, B. Zhang, X. Lu, X. Zhang, H. Zhu and B. Li, *Catal. Sci. Technol.*, 2018, **8**, 6180–6195.
32 J. Boltersdorf, N. King and P. A. Maggard, *CrystEngComm*, 2015, **17**, 2225–2241.
33 D. E. Scaife, *Sol. Energy*, 1980, **25**, 41–54.
34 H. Kato and A. Kudo, *J. Phys. Chem. B*, 2001, **105**, 4285–4292.
35 K. Maeda, D. Lu, K. Teramura and K. Domen, *J. Mater. Chem.*, 2008, **18**, 3539–3542.
36 K. Maeda, D. Lu, K. Teramura and K. Domen, *Energy Environ. Sci.*, 2010, **3**, 470–477.
37 H. Lyu, T. Hisatomi, Y. Goto, M. Yoshida, T. Higashi, M. Katayama, T. Takata, T. Minegishi, H. Nishiyama, T. Yamada, Y. Sakata, K. Asakura and K. Domen, *Chem. Sci.*, 2019, **10**, 3196–3201.